DOI: 10.1002/anie.200701173

Microencapsulation

Shell-in-Shell Microcapsules: A Novel Tool for Integrated, Spatially Confined Enzymatic Reactions**

Oliver Kreft, Michelle Prevot, Helmuth Möhwald, and Gleb B. Sukhorukov*

Efficient systems for protection and controlled release of encapsulated materials are highly sought-after techniques in fields like medicine, food technology, biotechnology, or materials science. Among other systems, such as micelles,[1,2] hydrogels,[3,4] and polymeric micro- and nanoparticles[5,6] (just to mention a few), hollow polyelectrolyte microcapsules offer a simple, inexpensive and gentle technique to encapsulate delicate biomaterials like enzymes, nucleic acids, and vaccines.[7,8] However, sustained separation of several components within confined compartments of a single capsule entity could not be achieved, yet. Existing multicompartment systems, such as polymeric micelles,[9] hybrid polymer microspheres,[10] two-compartment vesicles,[11] or even polyelectrolyte capsules hierarchically templated on melamine formaldehyde and silica,[12] have limitations in some significant applications owing to nonbiofriendly processing techniques, a low loading capacity, or the lack of permeability towards small solutes, such as substrates for biochemical processes or analytes for diagnostic tests. A capsule-in-capsule system built stepwise from semipermeable polyelectrolyte membranes and loaded with biomolecules under mild reaction conditions could be a solution to these problems.

The fabrication of polyelectrolyte capsules is based on the layer-by-layer (LbL) self-assembly of polyelectrolyte thin films.[13] Such capsules are fabricated by the consecutive adsorption of alternating layers of positively and negatively charged polyelectrolytes onto sacrificial colloidal templates.[7,14,15] Spherical calcium carbonate microparticles as a novel category of template have recently been described by us and others. This nontoxic template can be produced in the size range of 2 to 8 μm. It provides excellent loading capacities for biological materials together with rather "biofriendly" processing techniques, as it can be easily and gently removed by complexation with ethylenediaminetetraacetic acid (EDTA) after the build-up of the polyelectrolyte multilayer (PEM).[16–19] The semipermeability of the polyelectrolyte membrane allows small molecules (like EDTA, inorganic ions, and dyes) to enter and leave the capsule interior freely, whereas large molecules are retained.[20] In general, encapsulation of biomolecules offers several advantages: Encapsulated substances are protected against mechanical damage or degradation by hydrolytic enzymes;[21] furthermore, the accessibility of small molecules to encapsulated enzymes can be modulated as the small molecules must enter and leave the capsules to react with the biomolecules in the interior.[7,22,23]

Herein, we present a general method for the preparation of micrometer-sized shell-in-shell polyelectrolyte capsules. Our technique involves the fabrication of spherical ball-in-ball particles consisting of two concentric calcium carbonate compartments that can be independently loaded with biopolymers. Through deposition of polyelectrolyte multilayers, these ball-in-ball particles can be employed for the fabrication of completely novel capsule-in-capsule systems containing biomolecules separated by a semipermeable membrane.

We first demonstrate our concept by the encapsulation of two human serum albumin (HSA) species with different fluorescence labels as model biopolymers. Figure 1 illustrates the six steps involved in the formation of shell-in-shell capsules. Step 1 comprises the immobilization of tetramethylrhodamineisothiocynate (TRITC)–HSA and magnetite nanoparticles within spherical calcium carbonate microparticles by so-called coprecipitation.[24] On this precursor, we employed a PEM build-up by adsorbing five bilayers of polystyrene sulfonate (PSS) and polyallylamine hydrochloride (PAH; step 2). The resulting core–shell particles were subjected to a second coprecipitation step, this time in the presence of HSA labeled with Alexa Fluor 488 (step 3), leading to "ball-in-ball particles (type I)". These particles are characterized by a polyelectrolyte multilayer that is "sandwiched" between two calcium carbonate compartments. The second coprecipitation step was accompanied by the formation of single core $CaCO_3$ particles filled with Alexa–HSA. Owing to the magnetic properties of the inner compartment, it was possible to collect the Alexa–HSA particles by applying a magnetic field while all the nonmagnetic coproducts could be removed by a few washing steps (step 4; see Figure S1 in the Supporting Information).[25] "Ball-in-ball particles (type II)" were finally obtained by depositing a terminal PSS/PAH-multilayer (step 5). Scanning electron microscope (SEM) images illustrate that our approach to concentrically build up a calcium carbonate deposit on an initial calcium carbonate template was successful (Figure 2). The ball-in-ball particles had a total size ranging from 8–

[*] Dr. O. Kreft, Dr. M. Prevot, Prof. Dr. H. Möhwald
Max-Planck-Institut für Kolloid- und Grenzflächenforschung
Wissenschaftspark Golm, 14424 Potsdam (Germany)
Fax: (+49) 331-567-9222
E-mail: oliver.kreft@mpikg.mpg.de
Prof. Dr. G. B. Sukhorukov
Department of Materials
Queen Mary University of London
Mile End Road, E1 4NS, London (UK)

[**] The support by the Volkswagen Foundation (I/80 051-054) and the 6th FP EU projects STREP-NMP3-CT-2005-516922 "SelectNANO" and STREP-001428 "Nanocaps" is kindly acknowledged. We are grateful to Radostina Georgieva for fruitful discussions and to Jürgen Hartmann for assistance with SEM measurements.

Supporting information for this article is available on the WWW under http://www.angewandte.org or from the author.

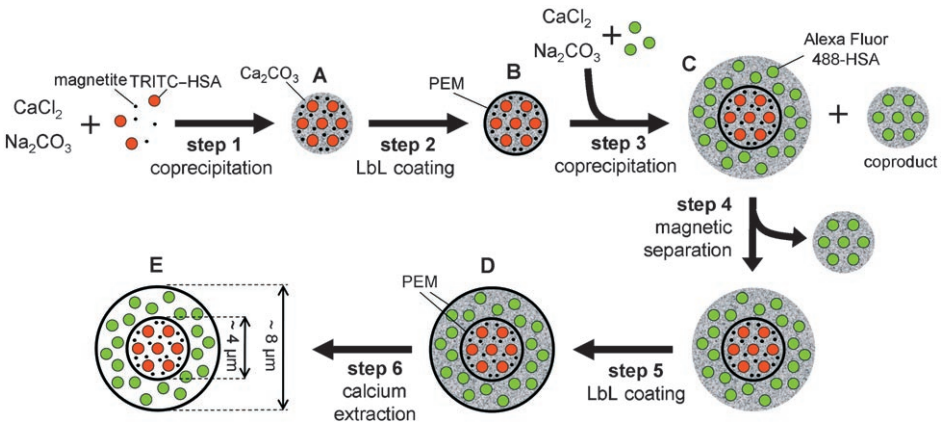

Figure 1. General route for the synthesis of shell-in-shell microcapsules. A = initial core; B = core–shell particle; C = ball-in-ball particle (type I); D = ball-in-ball particle (type II); E = shell-in-shell microcapsule.

10 µm with an inner core diameter of 3–4 µm. The cross section of a broken particle illustrates the radial symmetric character of the internal structure (Figure 2c,d). Both intersecting and terminating PEMs are clearly visible (Figure 2d).

EDTA treatment led to the dissolution of all calcium carbonate constituents and, thus, the formation a shell-in-shell capsule. During this treatment, the primarily immobilized HSA species were released into separate capsule compartments (Figure 1, step 6). This process was followed by a time series of confocal laser-scanning microscopy (CLSM) micrographs, which confirmed that mixing of both proteins was inhibited as the macromolecular biopolymers were retained by the intersecting polyelectrolyte shell (Figure 3, upper row). Recently, Lu et al. reported that the functionalization of $(PSS/PAH)_5$ capsules by embedding ferromagnetic gold/cobalt nanoparticles into the capsule shell increased the permeability towards high-molecular-weight dextran ($MW = 2 \times 10^6\ g\,mol^{-1}$) significantly.[23] However, we did not observe such an effect, which is presumably due the comparably low particle density (3000–5000 nanoparticles per capsule) in the present case. After being released from the calcium carbonate, parts of the Alexa–HSA particles (green color) adsorbed to the inner surface of the polyelectrolyte shell. This finding can be explained by strong electrostatic interactions between the polyelectrolyte shell and polar side chains of HSA. We believe that this effect is even intensified by the high surface area of the inner-capsule surface, which is a result of the highly porous geometry of the $CaCO_3$ template.[16,26] A series of simultaneously recorded transmission micrographs corroborates the existence of two individual polyelectrolyte capsules (Figure 3, lower row). Notably, upon calcium extraction, the inner capsule was able to move from the centre towards the shell of the outer capsule, indicating that calcium extraction leads to a disconnection of the inner capsule from the outer one (see the video in the Supporting Information.

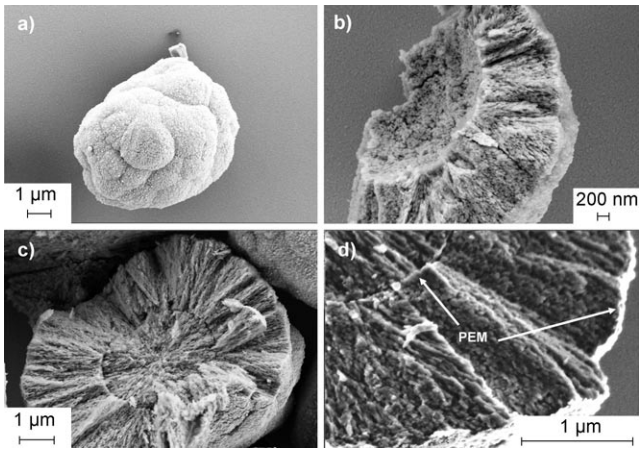

Figure 2. SEM micrographs of ball-in-ball particles (type II). Intact (a) and outer compartment (b) particles after mechanical particle rupture. c) Cross section of ball-in-ball particle. d) Cross section showing intersecting and enclosing PEMs (indicated by arrows).

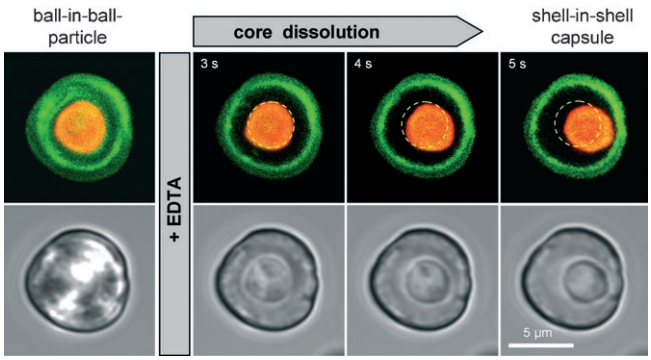

Figure 3. CLSM imaging of ball-in-ball (type II) particles during calcium extraction. Individual $CaCO_3$ compartments are loaded with TRITC–HSA (orange, inner) and Alexa Fluor 488–HSA (green, outer). After conversion into shell-in-shell capsules, both compounds remain separated owing to the intersecting polyelectrolyte shell. The dashed circle indicates the original position of the inner capsule moving to the outer shell upon calcium extraction.

Further to this rather conceptual work carried out with model proteins, we applied our strategy to a coupled bienzymatic system comprising glucose oxidase (GOD) and peroxidase (POD): Oxidation of glucose by GOD leads to the formation of H_2O_2, which, in the presence of an electron donor, acts as a substrate for POD (Figure 4a). As the electron donor, we have chosen Amplex Red, which is converted into the highly fluorescent resorufin by POD.[27] We encapsulated GOD in the outer surrounding compartment and POD in the inner capsule (Figure 4b). The coupling of both enzymatic reactions should be mediated by the semi-permeable character of the polyelectrolyte shell, which allows

small substrate (and product) molecules to diffuse in and out, whereas large enzyme molecules are retained in separated compartments. After adding glucose to the sample, H_2O_2 should be generated in the outer compartment (where GOD in located), but diffuse into both the bulk solution and the inner-capsule compartment thereafter. In contrast, resorufin formation is not initiated until Amplex Red is given to the sample and only takes place in the inner compartment (where POD is located). In agreement with our model, CLSM imaging in situ revealed that after successive addition of glucose and Amplex Red to the sample, resorufin fluorescence occurs within a few seconds in the inner compartment and then spreads into the outer compartment of the shell-in-shell structure (Figure 4c, video files visualizing the resorufin formation including control experiments are available in Figures S4–S6 in the Supporting Information). The apparent accumulation of resorufin reflects a steady-state concentration, which is determined by both the turnover rates of GOD and POD and the diffusion rates of H_2O_2 and resorufin through the inner polyelectrolyte membrane. However, we must emphasize that the coupled enzymatic test has mainly qualitative character.

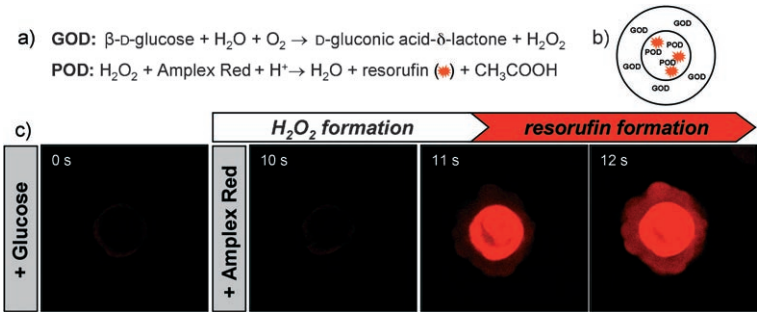

Figure 4. Coupled enzymatic test by using GOD and POD inside shell-in-shell capsules. a) Reaction schemes. b) Localization of GOD and POD within shell-in-shell capsules (for details, see Figure S2 in the Supporting Information. c) CLSM imaging in situ of resorufin formation.

Such two-compartment capsules exhibit exciting potential especially for biomedical applications: The separation between integrated components (e. g. enzyme and substrate, several cooperating enzymes, or even complex enzymatic cascade reactions) could be remotely removed, thus enabling a mixing and, hence, the start of a reaction by an external trigger. Remote opening systems based on ultrasound,[28,29] magnetic fields,[23] or IR lasers[30,31] have been recently demonstrated as well as the release through stimuli like pH, polarity, or ionic strength of the solvent.[32–35]

Experimental Section

PSS (MW = 70 kDa), PAH (MW = 70 kDa), TRITC–HSA (MW = 66000), GOD, POD (Sigma-Aldrich), and Amplex Red (Invitrogen) were used without any further purification. HSA labeled with Alexa Fluor 488 was synthetized according to the literature route[36] by using Alexa Fluor 488 carboxylic acid, succinimidyl ester *mixed isomers* (Invitrogen). Magnetite particles (diameter = 40 nm) were received from the Fraunhofer Institute of Applied Polymer Research (IAP, Potsdam-Golm, Germany).

Fabrication of calcium carbonate ball-in-ball particles and shell-in-shell capsules: $CaCO_3$ initial cores loaded with protein (TRITC–HSA or POD) and magnetite nanoparticles were prepared according to the previously described coprecipitation method.[24,37] Briefly, 1M $CaCl_2$ (0.615 mL), 1M Na_2CO_3 (0.615 mL), 1.4% (w/v) magnetite nanoparticle suspension (50 μL) and H_20 (2.450 mL) containing TRITC-HSA (2 mg or 0.5 mg POD) were rapidly mixed and thoroughly agitated on a magnetic stirrer for 20 s at room temperature. After the agitation, the precipitate was separated from the supernatant by centrifugation and washed three times with water. Resulting $CaCO_3$ particles (diameter = 4–6 μm) were coated with five bilayers of PSS and PAH by using the layer-by-layer assembling protocol[7] and subjected to a second coprecipitation step. In this second step, one-fourth of the coated initial cores was resuspended in 1M $CaCl_2$ (0.615 mL), 1M Na_2CO_3 (0.615 mL), and H_20 (2.500 mL) containing Alexa Fluor 488–HSA (1 mg or 0.5 mg GOD) and treated as described above. The resulting precipitate represents a mix of ball-in-ball particles (type I) and single cores that contain only Alexa 488–HSA. Magnetic ball-in-ball particles were isolated by applying an external magnetic field to the sample (see Figure S1 in the Supporting Information). We deposited 3000–5000 magnetite nanoparticles per calcium carbonate particle for this procedure. The ball-in-ball particles (type I) were coated with five bilayers of PSS and PAH according to the procedure described above, resulting in type-II ball-in-ball particles. The decomposition of the $CaCO_3$ particles by EDTA treatment was performed as previously described.[16] Enzymatic activities of GOD and POD were monitored in situ by CLSM after adding D-Glucose (50 mM) and Amplex Red (15 μM; in dimethyl sulfoxide).

Confocal images (CLSM) were recorded with a confocal laser-scanning system TCS SP DM IRB attached to an inverse microscope from Leica (Leica Microsystems, Wetzlar, Germany) that was equipped with a 100× oil-immersion objective with a numerical aperture of 1.4. Scanning electron microscopy (SEM) images were recorded by using a Gemini 1550 (Zeiss, Oberkochen, Germany) and an excitation voltage of 3.0 KeV. A drop of the capsule suspension was placed on a glass slide and allowed to dry at room temperature. Particles were crushed slightly to examine their interior. The particles were then sputter-coated with platinum to enable imaging with SEM.

Received: March 16, 2007
Published online: June 21, 2007

Keywords: materials science · microencapsulation · microreactors · multilayers · polyelectrolytes

[1] K. Kataoka, A. Harada, Y. Nagasaki, *Adv. Drug Delivery Rev.* **2001**, *47*, 113.
[2] V. P. Torchilin, *Cell. Mol. Life Sci.* **2004**, *61*, 2549.
[3] P. Gupta, K. Vermani, S. Garg, *Drug Discovery Today* **2002**, *7*, 569.
[4] Y. Qiu, K. Park, *Adv. Drug Delivery Rev.* **2001**, *53*, 321.
[5] A. Kikuchi, T. Okano, *Adv. Drug Delivery Rev.* **2002**, *54*, 53.
[6] H. H. Tonnesen, J. Karlsen, *Drug Dev. Ind. Pharm.* **2002**, *28*, 621.
[7] C. S. Peyratout, L. Dähne, *Angew. Chem.* **2004**, *116*, 3850; *Angew. Chem. Int. Ed.* **2004**, *43*, 3762
[8] A. G. Skirtach, O. Kreft, Stimuli-Sensitive Nanotechnology for Drug Delivery (Eds.: M. M. de Villiers, P. Aramwit, G. S. Kwon), in *Biotechnology: Pharmaceutical Aspects Series, Vol. 6*, AAPS Press, Virginia, USA, in press .

[9] A. F. Thünemann, S. Kubowicz, H. von Berlepsch, H. Möhwald, *Langmuir* **2006**, *22*, 2506.
[10] K. J. Pekarek, J. S. Jacob, E. Mathiowitz, *Nature* **1994**, *367*, 258.
[11] P. Y. Bolinger, D. Stamou, H. Vogel, *J. Am. Chem. Soc.* **2004**, *126*, 8594.
[12] Z. F. Dai, L. Dähne, H. Möhwald, B. Tiersch, *Angew. Chem.* **2002**, *114*, 4191; *Angew. Chem. Int. Ed.* **2002**, *41*, 4019.
[13] G. Decher, *Science* **1997**, *277*, 1232.
[14] E. Donath, G. B. Sukhorukov, F. Caruso, S. A. Davis, H. Möhwald, *Angew. Chem.* **1998**, *110*, 2323; *Angew. Chem. Int. Ed.* **1998**, *37*, 2201.
[15] G. B. Sukhorukov, E. Donath, S. Davis, H. Lichtenfeld, F. Caruso, V. I. Popov, H. Möhwald, *Polym. Adv. Technol.* **1998**, *9*, 759.
[16] D. V. Volodkin, N. I. Larionova, G. B. Sukhorukov, *Biomacromolecules* **2004**, *5*, 1962.
[17] C. Y. Wang, C. Y. He, Z. Tong, X. X. Liu, B. Y. Ren, F. Zeng, *Int. J. Pharm.* **2006**, *308*, 160.
[18] B. G. De Geest, R. E. Vandenbroucke, A. M. Guenther, G. B. Sukhorukov, W. E. Hennink, N. N. Sanders, J. Demeester, S. C. De Smedt, *Adv. Mater.* **2006**, *18*, 1005.
[19] J. Q. Brown, M. J. McShane, *IEEE Sens. J.* **2005**, *5*, 1197.
[20] O. Kreft, R. Georgieva, H. Bäumler, M. Steup, B. Müller-Röber, G. B. Sukhorukov, H. Möhwald, *Macromol. Rapid Commun.* **2006**, *27*, 435.
[21] O. P. Tiourina, A. A. Antipov, G. B. Sukhorukov, N. L. Larionova, Y. Lvov, H. Möhwald, *Macromol. Biosci.* **2001**, *1*, 209.
[22] Y. Lvov, A. A. Antipov, A. Mamedov, H. Möhwald, G. B. Sukhorukov, *Nano Lett.* **2001**, *1*, 125.
[23] Z. H. Lu, M. D. Prouty, Z. H. Guo, V. O. Golub, C. Kumar, Y. M. Lvov, *Langmuir* **2005**, *21*, 2042.
[24] A. I. Petrov, D. V. Volodkin, G. B. Sukhorukov, *Biotechnol. Prog.* **2005**, *21*, 918.
[25] D. V. Andreeva, D. A. Gorin, D. G. Shchukin, G. B. Sukhorukov, *Macromol. Rapid Commun.* **2006**, *27*, 931.
[26] D. V. Volodkin, A. I. Petrov, M. Prevot, G. B. Sukhorukov, *Langmuir* **2004**, *20*, 3398.
[27] N. G. Balabushevich, O. P. Tiourina, D. V. Volodkin, N. I. Larionova, G. B. Sukhorukov, *Biomacromolecules* **2003**, *4*, 1191.
[28] B. G. De Geest, A. G. Skirtach, T. R. M. De Beer, G. B. Sukhorukov, L. Bracke, W. R. G. Baeyens, J. Demeester, S. C. De Smedt, *Macromol. Rapid Commun.* **2007**, *28*, 88.
[29] D. G. Shchukin, D. A. Gorin, H. Möhwald, *Langmuir* **2006**, *22*, 7400.
[30] A. G. Skirtach, A. M. Javier, O. Kreft, K. Köhler, A. P. Alberola, H. Möhwald, W. J. Parak, G. B. Sukhorukov, *Angew. Chem.* **2006**, *118*, 4728; *Angew. Chem. Int. Ed.* **2006**, *45*, 4612.
[31] A. G. Skirtach, C. Dejugnat, D. Braun, A. S. Susha, A. L. Rogach, W. J. Parak, H. Möhwald, G. B. Sukhorukov, *Nano Lett.* **2005**, *5*, 1371.
[32] A. A. Antipov, G. B. Sukhorukov, Y. A. Fedutik, J. Hartmann, M. Giersig, H. Möhwald, *Langmuir* **2002**, *18*, 6687.
[33] K. Itano, J. Y. Choi, M. F. Rubner, *Macromolecules* **2005**, *38*, 3450.
[34] T. Mauser, C. Dejugnat, H. Möhwald, G. B. Sukhorukov, *Langmuir* **2006**, *22*, 5888.
[35] Z. J. Sui, J. B. Schlenoff, *Langmuir* **2004**, *20*, 6026.
[36] R. P. Haugland, *Handbook of Fluorescent Probes and Research Biochemicals*, Molecular Probes, Eugene, **2004**.
[37] G. B. Sukhorukov, D. V. Volodkin, A. M. Günther, A. I. Petrov, D. B. Shenoy, H. Möhwald, *J. Mater. Chem.* **2004**, *14*, 2073.

